



Structural characterization and hardness of carbon nanotube/alumina composites prepared by tri-sec-butoxide

Yemmani Suresh Babu*, Syed Altaf Hussain^b, B.Durga Prasad^c

^aPh.D. Research Scholar, Mechanical Department, Jawaharlal Nehru Technological University Anantapur, Ananthapuramu, Andhra Pradesh-515002, India.

^bProfessor & Mechanical Department, Rajeev Gandhi Memorial College of Engineering and Technology, Nandyal, Andhra Pradesh,-518501, India.

^cProfessor, Mechanical Department, Jawaharlal Nehru Technological University Anantapur, Ananthapuramu, Andhra Pradesh, India.

Corresponding Author Email: yemmanisuresh@gmail.com (Yemmani Suresh Babua)

Abstract:-

The so-gel approach was used in the production of an alumina matrix composite that had carbon nanotube reinforcement. On alumina powders, the effects of carbon nanotubes (CNTs) of varying concentrations—1%, 3%, 5%, 7%, and 9% weight were investigated. The findings indicate that reinforcing the material with CNTs at a weight of 1% was responsible for the improvement in wear resistance and hardness. The addition of carbon nanotubes to an alumina matrix composite led to an improvement in the material's hardness. This was caused by an enhanced load distribution brought about by the nanotubes' uniform distribution. A homogenous distribution of CNTs inside the Al₂O₃ matrix and a robust interfacial contact between CNTs and Al₂O₃ are necessary conditions for the fabrication of composites with better wear characteristics.

Key words: - Mixture of Al₂O₃/CNT; Pin-on-disc; Hardness, Wear rate, Water rate.

1. Introduction

Carbon nanotubes discovery has ushered in a new era of technological possibilities for transcending the limitations of conventional materials. Carbon nanotubes have the potential to be utilised as reinforcements in composite materials due to their extraordinary properties, such as an excellent Young's modulus, good flexibility, low density, and good electrical conductivity [1-2]. Metal matrix composites with graphene and carbon nanotube inclusions take use of the strength and charge carrier mobility of carbon nanostructures [3]. For industrial needs, matrix reinforcements are incorporated. Cheap reinforcements and different manufacturing procedures provide composites with desirable physical and mechanical qualities [4].

Acharyulu et al. (2020) report on an easy approach that is beneficial to the environment for the manufacture of carbon spheres (CS), titanium dioxide (TiO₂), and zinc oxide (ZnO) hollow structures. Krishnan et al. (2021) reported to reinforcement shifts XRD peaks towards lower 2theta values and changes intensity. As doping increases, interplanar distance (0-1-2) increases [6]. Jagadeesan et al. (2019) the nano magnesium oxide-carbon composite removes anthracene from actual effluent efficiently and environmentally. Optimal adsorption efficiency deviated 3.02% from expected experimental values [7]. In addition to magnesium and copper, catalytic cracking of methane at a temperature of 800 °C and a feed gas flow rate

of 20 mL/min is required for the synthesis of hydrogen and nano-carbon [8]. Lee et al. (2021) researchers looked at how incorporating even modest quantities of multi-walled carbon nanotubes (MWCNTs) into materials based on cement altered the thermal and electrical properties of the composites was investigated. They found that a connection between the electrode and the power source allowed them to deliver a consistent voltage, which allowed for the measurement of the temperature change that occurred in each specimen. The number of days that the MWCNTs cementitious composite was allowed to cure led to an increase in the amount of heat that it produced. In addition, the amount of heat that was generated by the composite rose in a manner that followed a quadratic shape as the concentration of MWCNTs increased [9]. Al- Rub et al. (2012) tested cementitious composites using MWCNTs. Based on aspect ratio, MWCNTs were long or short. MWCNT concentrations were 0.04 wt%, 0.1 wt%, and 0.2 wt% relative to cement. Curing times were 7, 14, and 28 days. After 28 days, MWCNT cementitious composites demonstrated higher flexural strength and ductility than conventional composites. Long MWCNTs performed similarly to short ones at low concentrations. After 28 days curing, the cementitious composite with 0.2 wt% short MWCNTs had the greatest physical attributes. The nano-engineered cementitious composite's physical properties improved because the short MWCNTs distributed efficiently and filled nano-sized pores [10]. Konsta-Gdoutos et al. (2014) tested cementitious composites with CNTs and CNFs for self-sensing. Electrical resistance and periodic loading with carbon nanomaterial concentrations of 0.1 and 0.3 wt% relative to cement assessed piezo resistance. 0.1 wt% CNT nano-engineered cementitious composite performed best electrically [11].

The purpose of this study was to determine how the wear characteristics and hardness of Al₂O₃-CNT composites were affected by varying concentrations of CNT, namely 1%, 3%, 5%, 7%, and 9%. The structural features of composites, as well as their interfacial connections, will be addressed when they are subjected to the conditions of the metal so-gel process.

2. Material and experimental method

2.1 Process of composite material

Carbon nanotube-enhanced alumina composite. Alumina precursor was aluminium tri-sec-butoxide (Al (OBus) 3). Alumina-supported catalyst and CVD produced 15–30 nm, 10–50 nm, and 1.6 g/cm³ multi-wall carbon nanotubes. The Yoldas process hydrolyzes and peptizes AlOOH to make alumina sol [12-13]. The alumina sol was mixed with alcohol-dispersed carbon nanotubes [14]. CNT volume fractions were 1, 3, 5, 7, and 9%. Six hours at 3500 dried carbon nanotube-alumina gel. Figure 1 shows the carbon nanotube/alumina composite powders made by calcining gel powder at 1250°C for 1 hour under 10 Pa vacuum. Electrical resistance and periodic loading with carbon nanomaterial concentrations of 0.1 and 0.3 wt% relative to cement assessed piezo resistance. 0.1 wt% CNT nano-engineered cementitious composite performed best electrically.

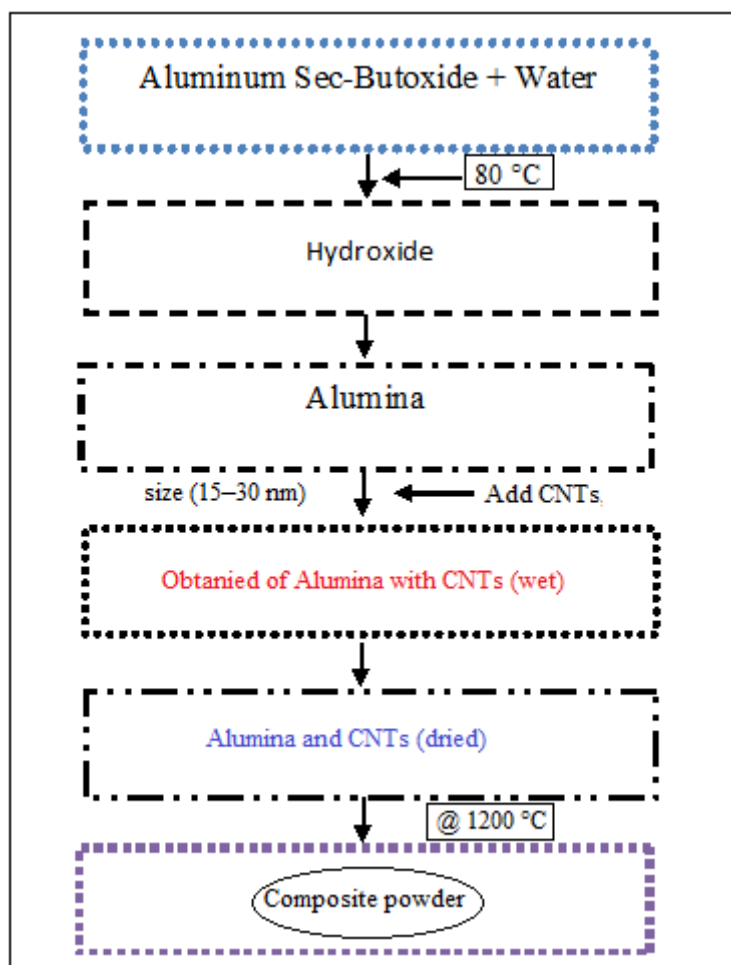


Figure 1. Process.

2.2. Characterization of composites

Spark plasma sintering allowed the calculated carbon nanotube/alumina powders to be mixed by Joule heat and spark plasma by a strong electric current. Spark plasma sintering removes powder surface oxides, allowing the powder compact to be sintered at a lower temperature. Calculated carbon nanotube/alumina particles were sintered in a graphite mould at 1650°C for 5 minutes under 25 MPa pressure. Spark plasma sintered carbon nanotube/alumina was annealed at 1000°C for 6 hours to remove graphite mould carbon. The fracture toughness of a carbon nanotube reinforced alumina matrix composite was measured by measuring the crack length formed. Figures 1 and 2 illustrate the samples and machining process.

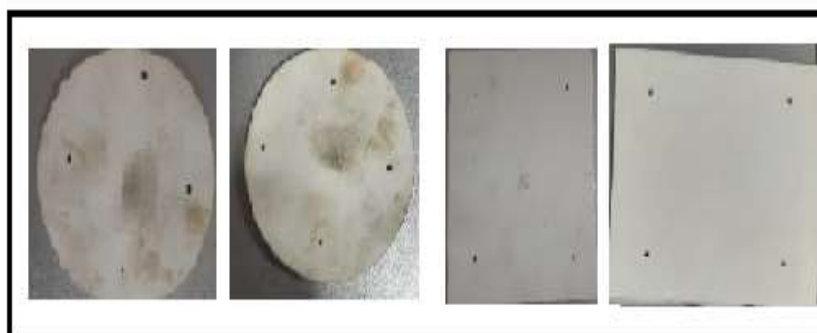


Figure 2. Samples.

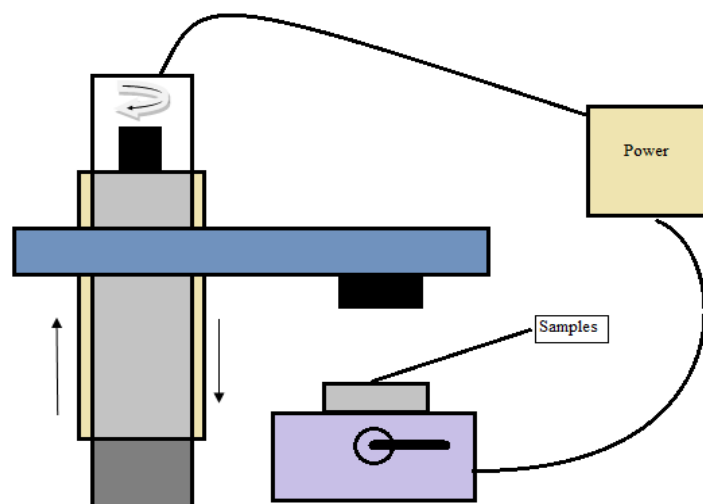


Figure 3. Machining process.

3. Results and discussion

Micro hardness measured specimen surface hardness. A pin-on-disc system tested wear resistance of generated samples. Flat composite samples were tested for wear resistance using ASTM standards. To assess abrasion, the samples were examined under an optical microscope after testing. This study examines how process factors like CNT wt. of 1, 3, 5, 7 and 9 %, rotational speed, normal load, and duration affect the wear behaviour of $\text{Al}_2\text{O}_3/\text{CNT}$ composites. A response surface model was used to investigate process parameters impacts on $\text{Al}_2\text{O}_3/\text{CNT}$ wear in Figures 4 to Figure 9. These graphs keep one parameter fixed at the middle level while the others change naturally.

3.1 Wear and water rate behaviour of $\text{Al}_2\text{O}_3/\text{CNT}$ with load

The load level is the most important component that plays a role in influencing the wear behaviour of $\text{Al}_2\text{O}_3/\text{CNT}$ as shown in Fig. 4. In general, the intensity of the usual load will cause the specimen to wear more quickly as it is increased. The work pieces hardness is another factor that influences wear and tear. The effect of normal load on wear is investigated under dry circumstances for a range of different CNT weight percentages in alumina. The graph that shows the relationship between normal load and wear may be produced by holding time and rotational speed at a constant level in the centre. In order to plot the graphs, the response surface model is used [15-16]. Figure depicts how the normal load has an effect on the dry sliding wear behaviour as well as the weight percent of CNT in alumina. Because of the increase in the normal load, the contact area that the specimen has with the counter disc will expand. This will cause heat to be generated between the contact surfaces, which will lead to the creation of micro grooves in the direction that the specimen is sliding. More wear is caused because of the small plastic deformation that can be seen at grooves and craters that are evident without fractures. This may be seen on the surface of the object. Figure 4 shows that for all wt. % of reinforcement, wear increases as the normal load increases. For 9% of CNT at low loads of A, the value of wear is $20\ \mu\text{m}$ and 1% of CNT at higher loads of E, high wear is observed ($126\ \mu\text{m}$). The presence of CNT particles dispersed on the pins surface and the construction of a secure layer between the pin and steel disc allow the wear to be reduced. By raising the weight percentage of CNT, specially created composites exhibit reduced wear. Similar results also found a similar outcome after adding CNT-reinforced particles to an alumina matrix material [17-18].

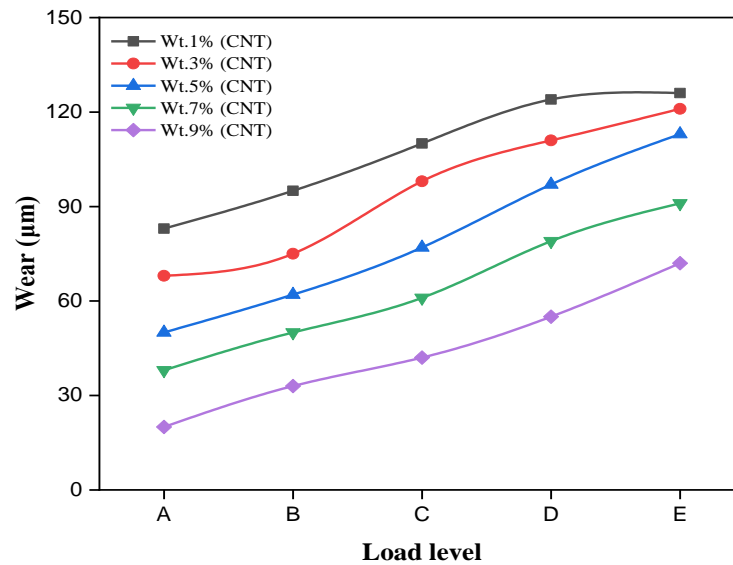


Figure 4. Variation of wear vs load.

Figure 5 illustrates the change in wear rate over time with regard to the usual load on Al₂O₃/CNT that was taken into consideration throughout this experiment. It can be deduced from the plot that, for all of the AMCs that were taken into consideration for this inquiry, the rate of wear is steadily rising with the rise in the usual load [19-20]. When a load of C is applied, the wear rate increases until it reaches its maximum value, after which it begins to gradually decrease. At 9 weight percent of CNT reinforced alumina, the wear rate at greater load is measured at 30.2 mm³/m, while at 1 weight percent of CNT alumina composites, the wear rate at higher load is measured at 37.89 mm³/m.

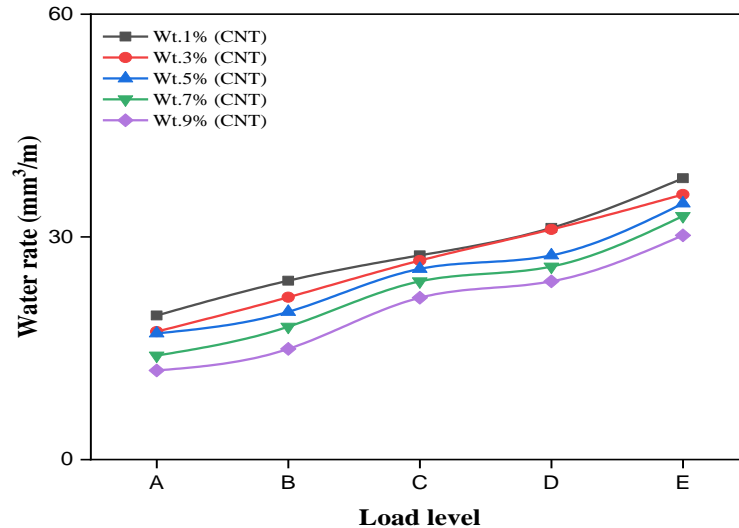


Figure 5. Variation of wear rate with load.

3.2 Effect of time on wear and water rate characteristics

Figure 6 and Figure 7 illustrate the wear and wear rate fluctuations experienced by all of the created composites throughout the course of time. These data may be taken into consideration for this inquiry since they are presented in graphical form. These displays were built by the use of the responses surface concept. As can be seen in Figure 6, the amount of wear and tear rises in a linear fashion as time passes. This is because there is less opportunity for contact to form when there is a high time requirement, which ultimately leads to produced composites experiencing less wear as a consequence. The 9% weight of CNT exhibits little to no wear after a maximum of 15 minutes of use.

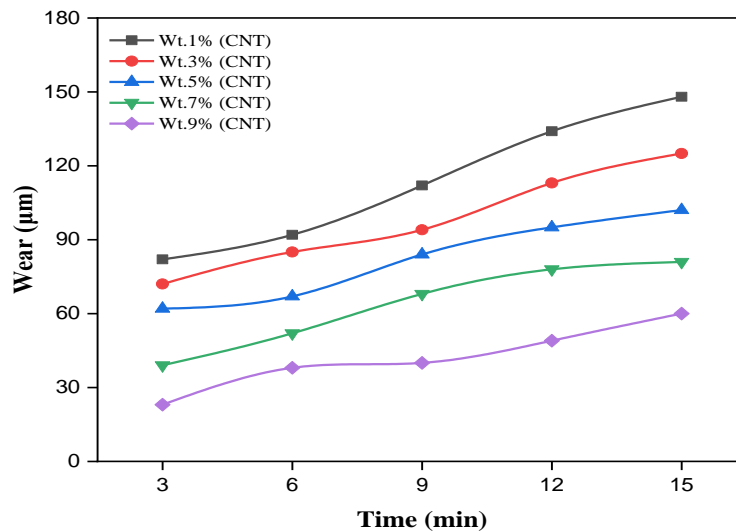


Figure 6. Variation of wear with time.

In figure 7, we see how the wear rate of Al₂O₃/CNT fluctuates throughout the course of time. It is possible to deduce from the graph that the trend for all weight percentages of CNT reinforced MMCs is upward, with the slope being the same as the passage of time rises. This is due to the fact that as the maximum duration increases, the temperature at the interface between the specimens and the disc also rises, which causes the base metal to become softer while simultaneously causing the reinforcing phase to de-bond. The surface of the sample will end up with craters and grooves as a consequence of this. The low wear rate is discovered to be 9 weight percent of CNT after a short period of time. The present experiment reveals that a substantial wear rate occurs at the maximum time condition for 1 weight percent of CNT.

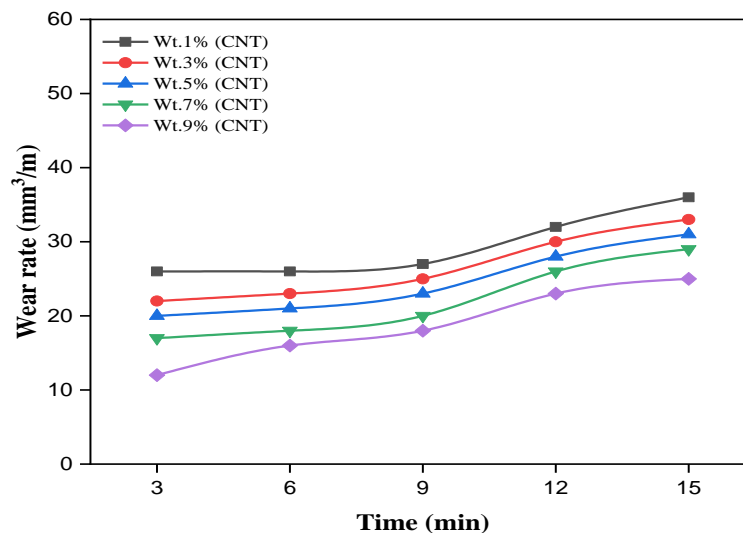


Figure 7. Variation of wear rate with time.

3.3 Effect of rpm on wear and water rate characteristics

The primary factor that determines how Al₂O₃/CNT will behave in terms of wear is the rotating speed. It's possible that this parameter's influence on wear characteristics will have a positive or a negative impact. Figure 8 illustrates the link between the rotational speed and wear on the component. The response surface model was used to produce this graph while the intermediate level parameters (other than rotational speed) were changed. Figure 8 shows that for all wt. % of CNT taken into account in this experiment, wear continuously decreases up to 600 rpm and thereafter increases. This may be the result of local plastic deformation at the location of the CNT particles under high-speed circumstances, which

causes surface delamination and sub-cracking. At a rotational speed of 600 rpm, 9 weight percent of CNT shows the least amount of wear. At 200 rpm of the disc speed, the wear rate for 1wt% of CNT is the highest

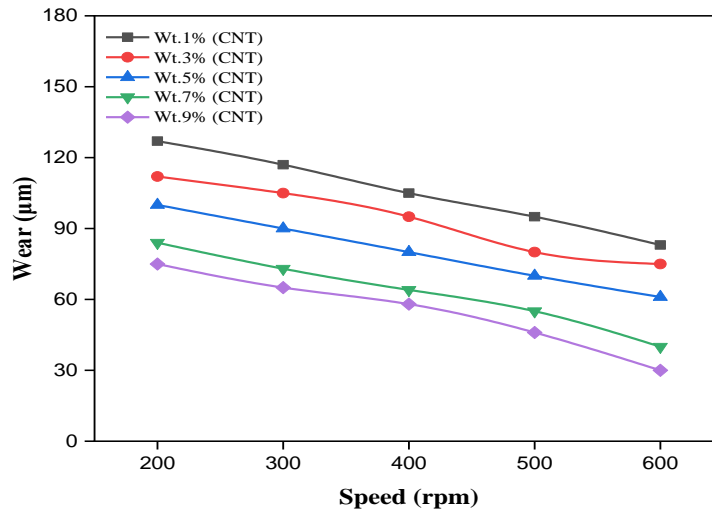


Figure 8. Variation of wear with speed.

The variations in wear rate with regard to rotational speed are shown in Figure 9 for all of the Al₂O₃/CNT that were taken into account for this investigation. When going from 200 to 600 revolutions per minute (rpm), the rotational speed results in a gradual reduction in the wear rate. This can be observed from the plot. When the pin spins swiftly, more material is lost from the surface because there is debris present at the point of contact between the pin and the surface. Additionally, cracks begin to form and spread throughout the surface of the pin. At a minimum rotational speed of 200 rpm, 9 weight percent of carbon nanotube (CNT) reinforced alumina exhibits the least amount of wear, while 1 weight percent of CNT exhibits the most amount of wear.

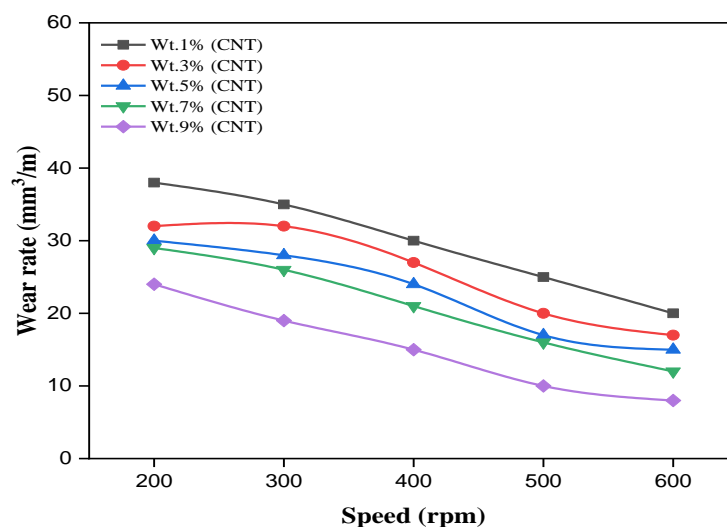


Figure 9 Variation of wear with speed.

4. Conclusions

The CNT/Al₂O₃ composite with an improved hardness may be successfully fabricated by using the Sol-gel technique in conjunction with spark plasma sintering. In the CNT/ Al₂O₃ experiment, the carbon nanotubes were distributed evenly throughout the alumina matrix. The relative brittleness of CNT/Al₂O₃ increased proportionally with the weight percent of carbon nanotubes. The CNT/Al₂O₃ load transfer is the basis upon which the strengthening process is built. In this line of study, the wear properties of composites made of Al₂O₃/CNT were investigated. Al₂O₃/CNT (reinforced with 1, 3, 5, 7 and 9 wt%

CNTs) exhibited increased wear resistance for low and moderate normal loads; however, for rotating speed, the 9 wt% CNT nanocomposite showed poor wear resistance. Al₂O₃/CNT was reinforced with 1, 3, 5, 7 and 9 wt% CNTs. The direct and indirect contributions of CNTs to the increased tribological properties of Al₂O₃/CNT composites were investigated. According to these results, nanocomposites with a high hardness and a very high resistance to wear would be excellent candidates for a wide range of technical applications.

References

1. Ardestani MS, Zaheri Z, Mohammadzadeh P, Bitarafan-Rajabi A, Ghoreishi SM. Novel manganese carbon quantum dots as a nano-probe: Facile synthesis, characterization and their application in naproxen delivery (Mn/CQD/SiO₂@naproxen). *Bioorg Chem* 2021; 115. <https://doi.org/10.1016/j.bioorg.2021.105211>
2. Paglia L, Genova V, Marra F, Bracciale MP, Bartuli C, Valente T, и съавт. Manufacturing, thermochemical characterization and ablative performance evaluation of carbon-phenolic ablative material with nano-Al₂O₃ addition. *Polym Degrad Stab* 2019; 169:108979. <https://doi.org/10.1016/j.polymdegradstab.2019.108979>
3. Ge X, Klingshirn C, Morales M, Wuttig M, Rabin O, Zhang S, и съавт. Electrical and structural characterization of nano-carbon–aluminum composites fabricated by electro-charging-assisted process. *Carbon N Y* 2021; 173:115–25. <https://doi.org/10.1016/j.carbon.2020.10.063>.
4. Hari Prasad M, Venkata Ramaiah P. Fabrication and characterization of Aluminum 6101-Selenium/boron carbide /carbon nanotubes metal matrix nano composites. *Mater Today Proc* 2022;66:1739–43. <https://doi.org/10.1016/j.matpr.2022.05.271>.
5. Acharyulu NPS, Babavali SKF, Srinivasu C. Nano structural transition metal oxide hollow spheres and carbon nano spherical structures by hydrothermal method and their characterization. *Mater Today Proc* 2020;27:1455–9. <https://doi.org/10.1016/j.matpr.2020.02.885>.
6. Krishnan SV, Ambalam MMM, Venkatesan R, Arivalagan M, Venkatachalapathy V, Mayandi J. Reinforcement of alumina with carbon nano cones and characterization. *Mater Today Proc* 2019; 35:57–61. <https://doi.org/10.1016/j.matpr.2019.05.442>.
7. Aravind Kumar J, Joshua Amarnath D, Anuradha Jabasingh S, Senthil Kumar P, Vijai Anand K, Narendrakumar G, и съавт. One pot Green Synthesis of Nano magnesium oxide-carbon composite: Preparation, characterization and application towards anthracene adsorption. *J Clean Prod* 2019;237. <https://doi.org/10.1016/j.jclepro.2019.117691>.
8. Alharthi AI, Alotaibi MA, Din IU, Abdel-Fattah E, Bakht MA, Al-Fatesh AS, и съавт. Mg and Cu incorporated CoFe₂O₄ catalyst: characterization and methane cracking performance for hydrogen and nano-carbon production. *Ceram Int* 2021; 47:27201–9. <https://doi.org/10.1016/j.ceramint.2021.06.142>.
9. Lee H, Seong J, Chung W. Effect of curing time on thermal response characterization of carbon-nano cementitious composites. *Compos Struct* 2021; 265:113781. <https://doi.org/10.1016/j.compstruct.2021.113781>.
10. Abu Al-Rub RK, Ashour AI, Tyson BM. On the aspect ratio effect of multi-walled carbon nanotube reinforcements on the mechanical properties of cementitious nanocomposites. *Constr Build Mater* 2012; 35:647–55. <https://doi.org/10.1016/j.conbuildmat.2012.04.086>.
11. Konsta-Gdoutos MS, Aza CA. Self-sensing carbon nanotube (CNT) and nanofiber (CNF) cementitious composites for real time damage assessment in smart structures.

- Cem Concr Compos 2014; 53:162–9. <https://doi.org/10.1016/j.cemconcomp.2014.07.003>.
12. Zhao W, Sun J, Huang Z. Three-dimensional graphene-carbon nanotube reinforced ceramics and computer simulation. *Ceram Int* 2021; 47:33941–55. <https://doi.org/10.1016/j.ceramint.2021.08.304>.
 13. Shin JH, Hong SH. Microstructure and mechanical properties of single wall carbon nanotube reinforced yttria stabilized zircona ceramics. *Mater Sci Eng A* 2012; 556:382–7. <https://doi.org/10.1016/j.msea.2012.07.001>.
 14. Anandaraj C, Venkatapathy R, Bharath Sabarish VC, Kalavani P, Durairajan A, Грача МР, и съавт. Structural characteristics, optical, electrical and electrochemical sensing properties of graphene and multi walled carbon nanotube admixed bismuth iron oxide composite ceramics. *Ceram Int* 2021; 47:28042–9. <https://doi.org/10.1016/j.ceramint.2021.06.141>.
 15. Ye F, Liang J, Cao Y, Song Q, Sui Y, Yang Z, и съавт. Cup-stacked carbon nanotubes hybridized Si₃N₄ / Si₃N₄ composite ceramics for high-efficiency microwave absorption with excellent thermal stability 2021; 47:15210–8.
 16. Venkataraman B, Sundararajan G. Correlation between the characteristics of the mechanically mixed layer and wear behavior of aluminum, Al-7075 alloy and Al-MMCs, *Wear* 245 (1–2) (2000) 22–38.
 17. D.H. Lu, M.Y. Gu, Z.L. Shi, Materials transfer and formation of mechanically mixed layer in dry sliding of metal composites against steel, *Tribology Letters* 6 (1) (1999) 57–61.
 18. Flahaut, E., Peigney, A., Laurent, C., Marlière, C., Chastel, F., & Rousset, A. (2000). Carbon nanotube–metal–oxide nanocomposites: microstructure, electrical conductivity and mechanical properties. *Acta Materialia*, 48(14), 3803–3812. Doi: 10.1016/s1359-6454(00)00147-6
 19. Go Yamamoto, Mamoru Omori, Kenji Yokomizo, Toshiyuki Hashida, Koshi Adachi. (2008). Structural characterization and frictional properties of carbon nanotube/alumina composites prepared by precursor method. *Nanotechnology*, 148(1-3) 265-269. <https://doi.org/10.1016/j.mseb.2007.09.013>
 20. Rivero-Antúnez P, Cano-Crespo R, Esquivias L, Rosa-Fox N de la, Zamora-Ledezma C, Domínguez-Rodríguez A, и съавт. Mechanical characterization of sol-gel alumina-based ceramics with intragranular reinforcement of multiwalled carbon nanotubes. *Ceram Int* 2020; 46:19723–30. <https://doi.org/10.1016/j.ceramint.2020.04.285>.